SINTEF
PROCEEDINGS
2

Proceedings of the 12th International Conference on Computational Fluid Dynamics in the Oil & Gas, Metallurgical and Process Industries

Progress in Applied CFD – CFD2017

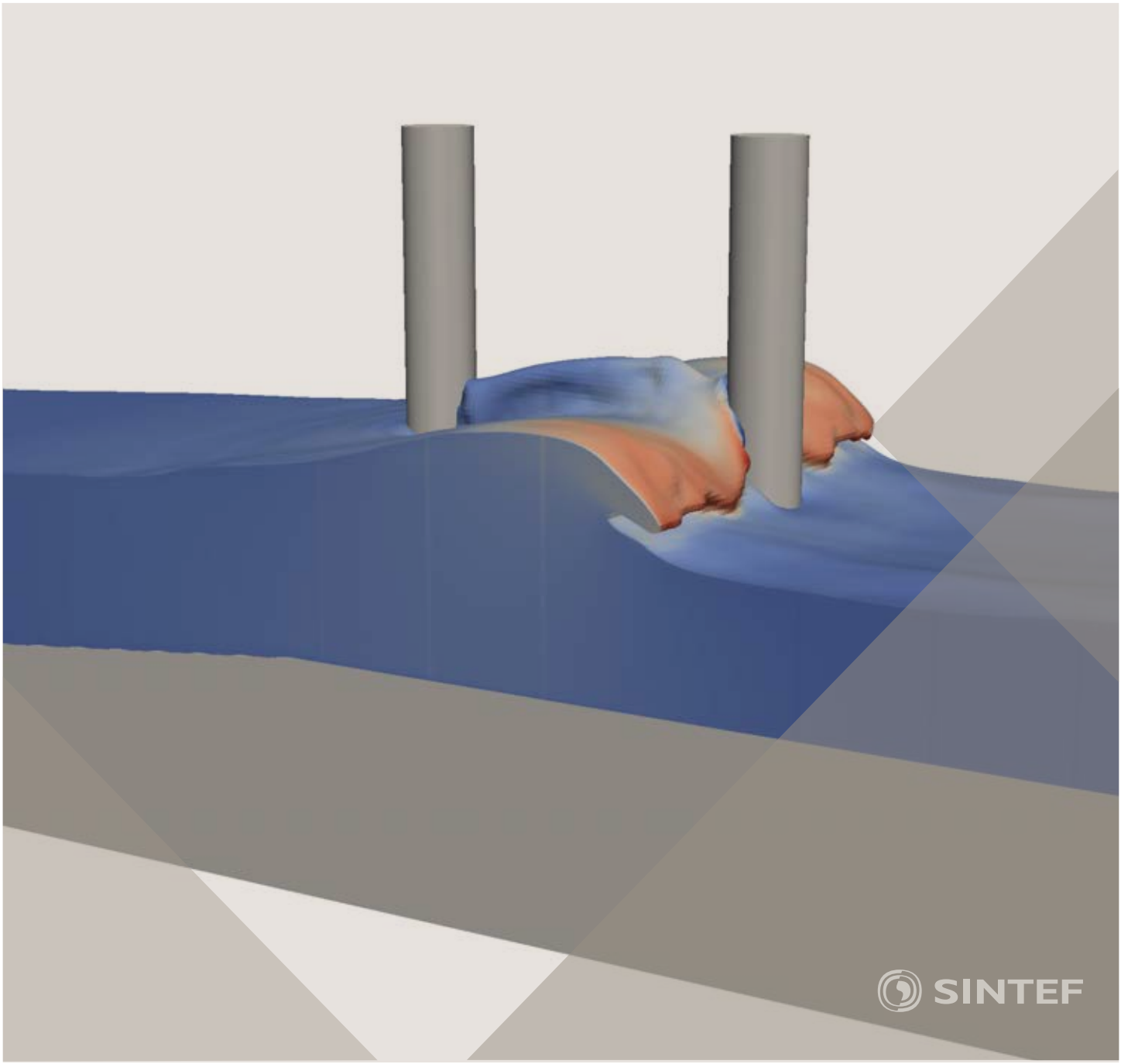

SINTEF Proceedings

Editors:
Jan Erik Olsen and Stein Tore Johansen

Progress in Applied CFD – CFD2017

Proceedings of the 12th International Conference on Computational Fluid Dynamics in the Oil & Gas, Metallurgical and Process Industries

SINTEF Academic Press

SINTEF Proceedings no 2
Editors: Jan Erik Olsen and Stein Tore Johansen
Progress in Applied CFD – CFD2017
Selected papers from 10th International Conference on Computational Fluid Dynamics in the Oil & Gas, Metallurgical and Process Industries

Key words:
CFD, Flow, Modelling

Cover, illustration: Arun Kamath

ISSN 2387-4295 (online)
ISBN 978-82-536-1544-8 (pdf)

SINTEF Academic Press
Address: Forskningsveien 3 B
PO Box 124 Blindern
N-0314 OSLO
Tel: +47 73 59 30 00
Fax: +47 22 96 55 08

www.sintef.no/byggforsk
www.sintefbok.no

SINTEF Proceedings
SINTEF Proceedings is a serial publication for peer-reviewed conference proceedings on a variety of scientific topics.
The processes of peer-reviewing of papers published in SINTEF Proceedings are administered by the conference organizers and proceedings editors. Detailed procedures will vary according to custom and practice in each scientific community.

PREFACE

This book contains all manuscripts approved by the reviewers and the organizing committee of the 12th International Conference on Computational Fluid Dynamics in the Oil & Gas, Metallurgical and Process Industries. The conference was hosted by SINTEF in Trondheim in May/June 2017 and is also known as CFD2017 for short. The conference series was initiated by CSIRO and Phil Schwarz in 1997. So far the conference has been alternating between CSIRO in Melbourne and SINTEF in Trondheim. The conferences focuses on the application of CFD in the oil and gas industries, metal production, mineral processing, power generation, chemicals and other process industries. In addition pragmatic modelling concepts and bio-mechanical applications have become an important part of the conference. The papers in this book demonstrate the current progress in applied CFD.

The conference papers undergo a review process involving two experts. Only papers accepted by the reviewers are included in the proceedings. 108 contributions were presented at the conference together with six keynote presentations. A majority of these contributions are presented by their manuscript in this collection (a few were granted to present without an accompanying manuscript).

The organizing committee would like to thank everyone who has helped with review of manuscripts, all those who helped to promote the conference and all authors who have submitted scientific contributions. We are also grateful for the support from the conference sponsors: ANSYS, SFI Metal Production and NanoSim.

Stein Tore Johansen & Jan Erik Olsen

Organizing committee:

Conference chairman: Prof. Stein Tore Johansen
Conference coordinator: Dr. Jan Erik Olsen
Dr. Bernhard Müller
Dr.Sigrid Karstad Dahl
Dr.Shahriar Amini
Dr.Ernst Meese
Dr.Josip Zoric
Dr.Jannike Solsvik
Dr.Peter Witt

Scientific committee:

Stein Tore Johansen, SINTEF/NTNU
Bernhard Müller, NTNU
Phil Schwarz, CSIRO
Akio Tomiyama, Kobe University
Hans Kuipers, Eindhoven University of Technology
Jinghai Li, Chinese Academy of Science
Markus Braun, Ansys
Simon Lo, CD-adapco
Patrick Segers, Universiteit Gent
Jiyuan Tu, RMIT
Jos Derksen, University of Aberdeen
Dmitry Eskin, Schlumberger-Doll Research
Pär Jönsson, KTH
Stefan Pirker, Johannes Kepler University
Josip Zoric, SINTEF

CONTENTS

12th International Conference on CFD in Oil & Gas, Metallurgical and Process Industries
SINTEF, Trondheim, Norway *CFD 2017*
May 30th – June 1st 2017

A NUMERICAL EVALUATION OF THE EFFECT OF ELECTRO-MAGNETIC FORCE ON BUBBLE FLOW IN ALUMINIUM SMELTING PROCESS

Yuqing FENG[1,*], Peter J. WITT[1], Zhibin ZHAO[1,2], Kaiyu ZHANG[3], M. Philip SCHWARZ[1], Zhaowen WANG[2]
[1] CSIRO Mineral Resources, Victoria 3169, AUSTRALIA
[2] NORTHEASTERN UNIVERSITY School of Metallurgy, Shenyang, CHINA
[3] Hefei University of Technology, CHINA

*E-mail: Yuqing.Feng@csiro.au

ABSTRACT

This paper aims to investigate the effect of electro-magnetic forces on bubble flow under an anode using a computational fluid dynamics (CFD) model with the volume-of-fluid (VOF) method to capture the gas-liquid interface. Current flow was solved simultaneously to determine the Lorentz forces. As an initial phase of investigation, the investigation was conducted using part of a single anode geometry as a test bed. The CFD model was run with a fixed bubble volume and two anode inclination angles. The effect of Lorentz forces was assessed in terms of bubble sliding velocities, bubble shapes and trajectories.

Keywords: CFD, Aluminium Electrolytic Cell, Bubble Flow, Electro-Magnetic Force.

NOMENCLATURE

Greek Symbols
α Volume fraction.
ρ Mass density, [kg m^{-3}].
ϕ Electric potential [V].
σ Electrical conductivity, [S m^{-1}].
μ Dynamic viscosity, [kg m^{-1} s^{-1}].

Latin Symbols
B Magnetic flux density, [T].
E Electric field, [V m^{-1}].
$\mathbf{F}_L$ Volumetric Lorentz force, [N m^{-3}].
$\mathbf{F}_S$ Surface tension force, [N m^{-3}].
g Gravity vector [m s^{-2}].
J Electric current density, [A m^{-2}].
p Pressure, [Pa].
t Time [s].
u Velocity, [m s^{-1}].

Sub/superscripts
g Gas.
l Liquid.

INTRODUCTION

Bubble flow is an inherent phenomena in Hall- Héroult reduction cells for aluminium smelting, and plays an import role in determining cell performance. A better understanding of the bubble dynamics and the resulting liquid flow is key to improving cell performance. Due to the corrosive and high temperature environment, bubble dynamics are traditionally studied using substitute physical models, including water models, low temperature electrolytic models, small-scale high-temperature electrolytic cells. A detailed summary of these models was made in a recent publication (Zhao et al., 2016a). Due to the limitation of measurement technology, the detailed bubble dynamics cannot be studied quantitatively in physical models at or near industrial scale. In the last decade, numerical modelling has been used increasingly to study bubble dynamics in the aluminium smelting system. These studies have focused on different areas, such as bubble detachment on the effect of aluminium-cryolite interfaces (Einarsrud, 2010), bubble detachment and sliding mechanism (Das et al., 2011), anode edge shape on bubble release (Wang and Zhang, 2010) and the effect of MHD forces on global bubble behaviour and voltage fluctuation (Einarsrud et al., 2012).

The CSIRO CFD team, in collaboration with a number of aluminium smelting companies, has developed a multi-scale CFD modelling approach to study bubble induced bath flow in aluminium smelting cells. This bath flow model (Feng et al., 2010, 2015) was developed using a local averaged approach accompanied with PIV measurement for model validation (Cooksey and Yang, 2006). To understand detailed bubble dynamics a micro-approach based on the Volume of Fluid (VOF) model was developed in parallel. Using the latter approach, for the first time, the difference in bubble dynamics between air-water and CO_2-cryolite systems were quantified for motion of a single bubble in the ACD (anode-cathode distance) and for continuous bubbles motion in side

channels (Zhang et al., 2013; Zhao et al., 2015). In the detailed bubble model the electro-magnetic force, or Lorentz force, was not included.

Bojarevics and Roy (2012) performed an analytical evaluation of the electro-magnetic force on a hemispherical stationary bubble under an anode, and suggested that the presence of the electro-magnetic force could significantly affect the bubble transport, concentration and detachment. In a recent physical model study using aqueous $CuSO_4$ electrolysis (Das et al., 2015), the superposition of a magnetic field significantly affected the bubble density, coalescence, velocity and the overall sliding characteristics. Using a multiscale modelling approach, Einarsrud et al (2012) found that the inclusion of Lorentz force did not appear to influence global bubble behaviour and voltage fluctuations significantly. However, the Lorentz force appeared to enhance bubble departure by 7 and 12% in the two cases they investigated. To quantitatively evaluate the effect of electric-magnetic force on bubble behaviour, it is necessary to simulate the motion of individual bubbles in three dimensions.

This paper aims to further investigate the effect of electro-magnetic forces on bubble flow under an anode using a computational fluid dynamics (CFD) model with the volume-of-fluid (VOF) method used to capture the gas-liquid interface. Current flow was solved simultaneously to determine the Lorentz force. The investigation was conducted using part of a single anode geometry as a test bed. The CFD model was run for a single bubble with fixed bubble volume and two anode inclination angles with different directions of the electro-magnetic field. The effect of Lorentz force was assessed in terms of bubble sliding velocities, bubble shape and trajectories.

MODEL DESCRIPTION

Gas-Liquid Flow Model

Transient fluid dynamics of the gas and liquid bath are simulated by solving transport equations for the conservation of mass and momentum. The governing equations for the two-phase mixture are:

Global continuity equation

$$\nabla \cdot \mathbf{u} = 0 \tag{1}$$

Momentum equation

$$\frac{\partial(\rho\mathbf{u})}{\partial t} + \nabla \cdot (\rho\mathbf{u}\mathbf{u}) = -\nabla p + \nabla \cdot [\mu(\nabla\mathbf{u} + \nabla\mathbf{u}^{\mathrm{T}})] + \rho\mathbf{g} + \mathbf{F}_s + \mathbf{F}_L \tag{2}$$

Mixture density and viscosity are weighted based on volume fraction in the following manner:

$$\rho = \alpha_g\rho_g + \alpha_l\rho_l \tag{3}$$

$$\mu = \alpha_g\mu_g + \alpha_l\mu_l \tag{4}$$

The interface location between the two phases is calculated using the volume of fluid (VOF) approach in which a transport equation for the gas volume fraction is solved.

Gas phase continuity equation

$$\frac{\partial(\rho_g\alpha_g)}{\partial t} + \nabla \cdot (\rho_g\alpha_g\mathbf{u}) = 0 \tag{5}$$

Electro-Magnetic Model

The Lorentz force in equation (2) is given by:

$$\mathbf{F}_L = \mathbf{J} \times \mathbf{B} \tag{6}$$

where the current density, **J**, is;

$$\mathbf{J} = \sigma(\mathbf{E} + \mathbf{u} \times \mathbf{B}) \tag{7}$$

noting that the electrical conductivity, σ, is phase weighted as the other fluid properties (e.g. density). Since the velocities are small the induced current term on the right hand side is small and ignored in this work. The electric field can be defined in terms of a scalar potential ($\mathbf{E} = -\nabla\emptyset$) then from equation (7) and current conservation the potential equation to be solved is:

$$\nabla \cdot (\sigma\nabla\emptyset) = 0 \tag{8}$$

Geometry and Boundary Conditions

The model geometry is a 0.15[m] wide three dimensional slice of a section of the anode and bath from a reduction cell. The model domain and boundary condition locations for the model are shown in Figure 1, consisting of a solid domain for the anode and fluid domain for the cryolite-CO_2 mixture. The brown slice is through the centre of the anode, which has a height of 0.4 [m] and a length of 0.65 [m] in Z and Y directions respectively. A uniform current density of 9 [kA m^{-2}] is applied to the top pink coloured surface.

A plane through the centre of the bath coloured, by volume fraction, shows the initial conditions for the blue CO2 and red cryolite fluids. The fluid domain consists of the volume under the anode in the ACD, which has a depth of 40 [mm], and the volume in the centre channel beside the anode. Centre channel half width is 0.12 [m] with the top light blue face set as an outlet boundary at zero gauge pressure. Initial liquid height in the centre channel is 0.15 [m] above the base of the bath. The grey base of the bath is a non-slip wall set at a fixed voltage of 0 [V] and represents the top surface of the metal pad in an operating cell. Two surfaces couple the anode and bath domains via conducting walls that allow current to pass between the domains. For the fluid side the flow boundary condition is a non-slip wall. The high and low x-direction surfaces are set as symmetry planes or effectively free-slip insulating walls. Other surfaces and insulated non-slip walls.

A small surface, 5 [mm] by 5 [mm] square and 0.07 [m] from the low y end of the anode, is located on the base of the anode. As detailed nucleation of the gas is not considered here, it is assumed that CO_2 gas enters the domain at this surface to form a bubble. Inclination of the anode is accounted for by altering the direction of the gravity vector.

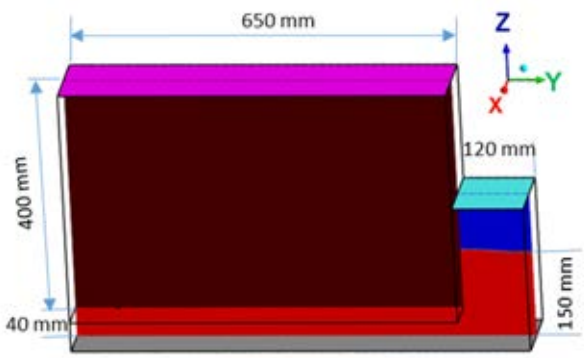

Figure 1: Schematic diagram of geometry.

Initially the domain is meshed using 620,000 hexahedral cells with 485,000 in the anode domain and 135,000 in the fluid domain. This cell size is consistent with our previous work in Zhao et al., (2015). To resolve details of the bubble interface three levels of adaptive meshing was used based on the gradient of volume fraction. Figure 2 shows the cut-cell mesh refinement around the bubble at 0.22 [s] with the green line indicating the gas-liquid interface. The grey surface in Figure 2 is in the X-Y (horizontal) plane and the colored surface is a Y-Z (vertical) plane. With mesh refinement the cell count increases to approximately 1.2 million cells with most of the increase being in the fluid domain.

Gas is added to cells adjacent to the 5 [mm] x 5 [mm] square "nucleation site" at a rate of $2.5x10^{-6}$ [kg s^{-1}] for a period of 0.16 seconds. Thus, a single bubble with an equivalent bubble size of 25.2 [mm] is formed, with an approximate thickness of 2 [mm]. For cases with a magnetic field, it was applied at a uniform strength of 0.02 [T] in either the x or y direction as defined in Figure 1.

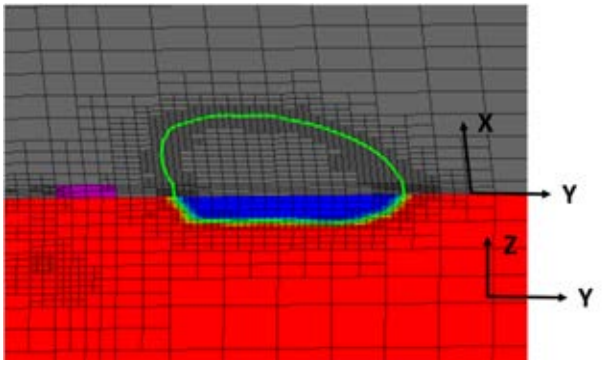

Figure 2: Mesh refinement around bubble at 0.22 [s], grey surface - anode base, blue - CO^2, .red - cryolite, pink – gas "nucleation site".

Material Properties

Properties were based on typical values for operating industrial cells as are summarised in Table 1.

Table 1: Physical Properties.

Cryolite Density	2100 [kg m^{-3}]
CO_2 Density	0.4 [kg m^{-3}]
Cryolite Dynamic Viscosity	0.003 [Pa s]
CO_2 Dynamic Viscosity	$1.37x10^{-5}$ [Pa s]
Cryolite-CO_2 Surface Tension	0.132 [N m^{-1}]
Contact angle Cryolite-CO_2	120°
Cryolite Electrical Conductivity	222 [S m^{-1}]
CO_2 Electrical Conductivity	1 [S m^{-1}]
Carbon Anode Electrical Conductivity	21,430 [S m^{-1}]

Solution Scheme

Model results were obtained using ANSYS-Fluent 17.1 to solve equations (1,2,5 and 8) in the fluid domain and equation (8) in the solid domain by a finite volume scheme. PISO is used for pressure velocity coupling and a second order upwind scheme used for momentum. A first order implicit transient scheme with adaptive time stepping is used for time advancement. The time step is determined by targeting a Courant number of 0.5, typically this results in a time step of 0.0002 seconds and approximately 8-12 iterations are required to converge each time step.

The location of the gas-liquid interface is predicted using the explicit VOF formulation and geometric reconstruction of the interface shape. Surface tension effects in equation (2) are calculated using the continuum surface force model with wall adhesion.

Equation (8) is solved as a user defined scaler equation with no transient or convective terms, using a second order central difference scheme. User defined functions are used to calculate the current density and Lorentz force. UDFs are also used to add mass source terms for gas nucleation at the base of the anode.

RESULTS

No Lorentz Force

To obtain a baseline for the bubble behaviour the model was run with no magnetic field and thus no Lorentz force. The gravity vector was orientated such that the base of the anode was sloping upward toward the centre channel at 1.5° to the horizontal. This being representative of an anode that has worn to the shape of a metal pad with significant heave.

Iso-surfaces showing the gas-liquid interface are plotted at a number of time instants in Figure 3. Results are plotted looking upward from the metal pad to the anode and from the side of the cell. The first image is at 0.16 seconds at the time that CO_2 gas stops entering the model.

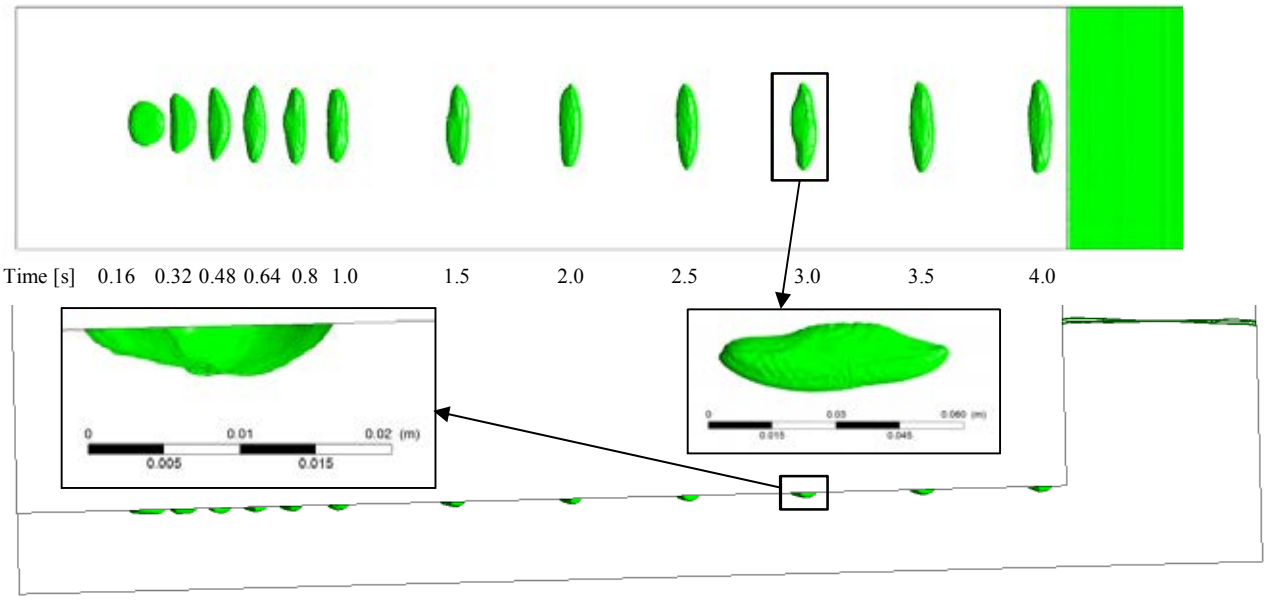

Figure 3: Bubble interface locations at various time instants with no Lorentz force a 1.5° anode slope, View from underneath (top) View from side (bottom). Insets shows details of the bubble shape and size at 3.0 seconds.

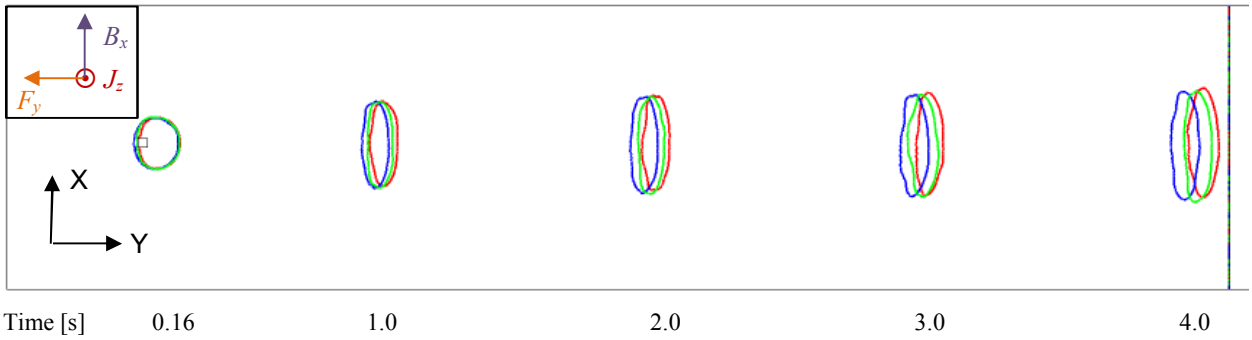

Figure 4: View from underneath of bubble outline at various time instants with a 1.5° anode slope and with — no Lorentz force, — B_x=-0.02 [T], — B_x=0.02 [T]. Inset shows direction of the fields and force for B_x=0.02 [T].

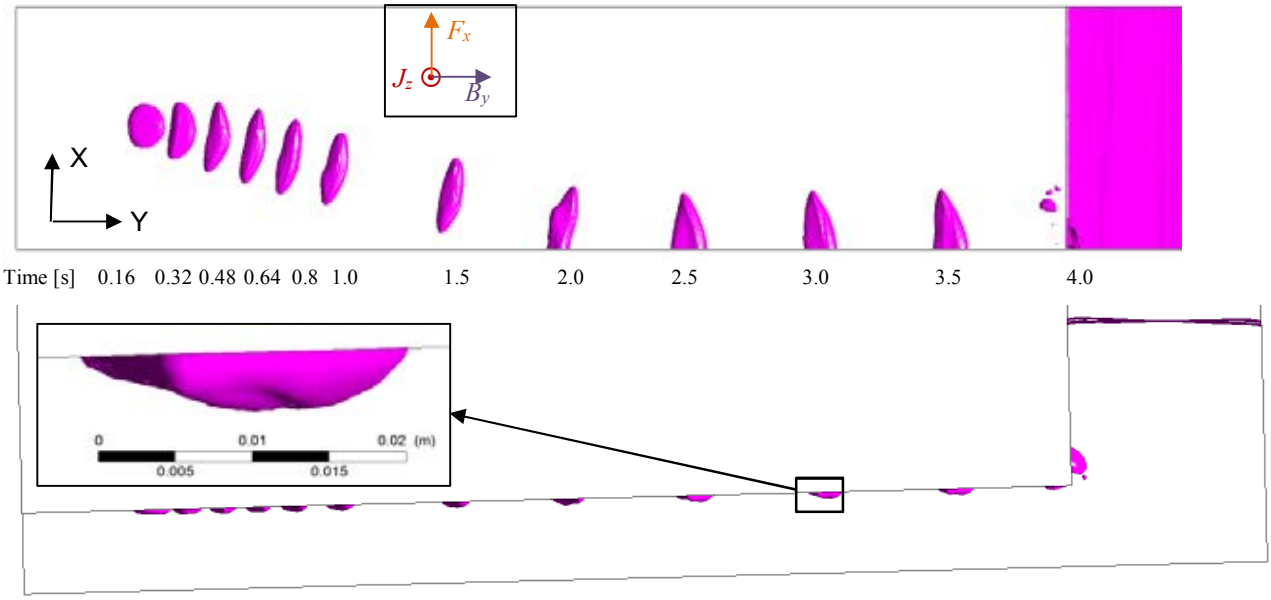

Figure 5: Bubble interface locations at various time instants with a 1.5° anode slope and a magnetic field of B_y=0.02 [T], View from underneath (top) View from side (bottom). Inset shows details of the bubble shape and size at 3.0 seconds.

Table 2: Predicted average bubble dimensions.

	Anode base angle 1.5°				Anode base angle 0.5°	
Magnetic Field	0	B_x=0.02 [T]	B_x=-0.02 [T]	B_y=0.02 [T]	B_x=0.02 [T]	B_x=-0.02 [T]
Width [m] (Y direction)	0.0149	0.0147	0.0146	0.0212	0.0196	0.0260
Length [m] (X direction)	0.0529	0.0528	0.0517	0.0372	0.0391	0.0297
Aspect Ratio	3.6	3.6	3.5	1.8	2.0	1.1
Velocity [m s^{-1}]	0.145	0.146	0.144	0.156	0.121	0.056
Thickness [mm]	1.99	2.00	2.00	2.24	1.88	1.75

At this time the bubble has moved under buoyancy to the right with the left edge of the bubble just exposing the edge of the nucleation site. As shown in previous work (Zhao *et al.*, 2015) the bubble is initially circular and deforms to a sausage bubble as it moves towards the centre channel under buoyancy.

Bubble dimensions obtained by averaging the bubble position at half second intervals between 1.5 and 3.5 seconds are given in Table 2. The predicted behaviour, thickness, aspect ratio and velocity are in agreement with those reported and validated by Zhao *et al.* (2015) for a similar system using a similar modelling methodology.

Effect of Transverse Magnetic Field

To identify if the Lorentz force has an effect on bubble motion, a magnetic field of 0.02 [T], typical of that found in industrial potlines, was applied in the x-direction and in the negative x-direction. From equation (6) for a downward current, J_z, and transverse magnetic field, B_x, the Lorentz force acts in the negative y-direction, away from the centre channel, as shown schematically in the top left of Figure 4. When the magnetic field is applied in the negative x-direction the force acts in the positive y-direction, towards the centre channel. Figure 4 shows the bubble position at four time instants for the case with no magnetic field and two cases with the magnetic field in the x-direction.

As evident by the results in Figure 4 and Table 2 the Lorentz force arising from B_x causes a small change in the bubble velocity and thus motion of the bubble with time.

Effect of Longitudinal Magnetic Field

Results from a simulation with the magnetic field acting in the y-direction are presented in Figure 5. Reorienting the magnetic field also changes the force direction with it now acting in positive x-direction. The bubble trajectory is plotted in Figure 5 and shows that the bubble is moved across the base of the anode and at approximately 2.0 seconds contacts the model boundary. In the model the boundary is effectively a free slip wall thus the bubble travels along the wall before rising along the anodes in the centre channel. From Table 2 the bubble length reduces and its thickness increases changing its profile and thus drag, resulting in an increased velocity. In a reduction cell this change would not occur and the bubble would continue traversing across the anode base until it reached a slot or edge of the anode.

Effect of Anode Base Angle

The two cases with the magnetic field in the positive and negative x-direction were run with the anode inclination angle reduced from 1.5° to 0.5°. Figure 6 shows plots of the bubble locations for the reduced inclination cases.

With the buoyancy force reduced, the Lorentz force has a stronger effect on the bubble. As shown in Table 2 and Figure 6, when the Lorentz force acts in the same direction as the buoyancy force on the bubble, the bubble velocity is reduced to half of that when compared to the case with the Lorentz force opposing to the buoyancy force.

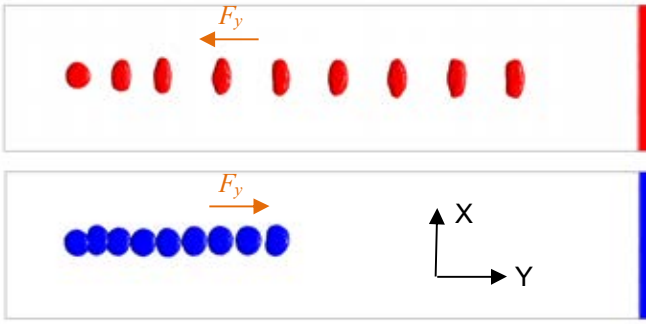

Figure 6: View from underneath of bubble interface locations at various time instants for a 0.5° anode slope and with Lorentz force of B_x=-0.02 [T] (bottom) and B_x=0.02 [T] (top). Time [s] from left to right are: 0.16 0.64 1.0 1.5 2.0 2.5 3.0 3.5 4.0.

CONCLUSION

Numerical simulations of CO_2 bubbles moving in cryolite bath under an anode in the presence of a magnetic and electric field were performed using a three dimensional VOF model. Results show that the Lorentz force produced by the electro-magnetic fields alters the behaviour of the CO_2 bubbles.

Bubbles are predicted to move in the direction opposing the MHD force acting on the liquid. For a case with the anode at an angle of 1.5° and a transverse magnetic field the effect on bubble motion was small. For the same geometry but when the magnetic field is aligned in the longitudinal direction of the anode the MHD force cause the bubbles to move transverse to their trajectory when only buoyancy is acting.

With a reduced anode inclination angle of 0.5° the MHD force had a strong influence on the bubble velocity with

the velocity varying between 0.056 and 0.121 [m s^{-1}] depending on the direction of the magnetic field.

This work demonstrates that the electro-magnetic force in aluminium reduction cells has the potential to alter the behaviour of gas bubbles.

ACKNOWLEDGEMENT

Zhibin Zhao and Kaiyu Zhang would like to thank the China Scholarship Council (CSC) and the National Natural Science Foundation of China (Grant No. 51529401) for their visiting Ph.D. scholarships to study at CSIRO.

REFERENCES

BOJAREVICS, V. and ROY, A., (2012), "Effect of magnetic forces on bubble transport and MHD stability of aluminium electrolysis cells", Magnetohydrodynamics, 48, 125-136.

COOKSEY, M.A. and YANG, W., (2006), "PIV measurements on physical models of aluminium reduction cells", Light Metals, 359-365.

DAS, S., MORSI, Y., BROOKS, G., YANG, W. and CHEN, J. J. J., "The principal characteristics of the detachment and sliding mechanism of gas bubble under an inclined anode", 10th Australasian Aluminium Smelting Technology Conference. Launceston, Tasmania, 2011.

DAS, S., WEERASIRI, L.D. and JEGATHEESAN, V., (2015), "Bubble flow in a static magnetic field", Light Metals 2015, 789-793.

EINARSRUD, K. E., (2010), "The effect of detaching bubbles on aluminum−cryolite interfaces: An experimental and numerical investigation", Metall. Mater. Trans. B., 41, 560.

EINARSRUD, K. E., Johansen, S. T. and Eric, I., (2012), "Anodic bubble behaviour in Hall-Heroult cells", Light Metals, 875-880.

FENG, Y.Q., YANG, W., COOKSEY, M. and SCHWARZ, M.P., (2010), "Development of Bubble Driven Flow CFD Model Applied for Aluminium Smelting Cells", *J. Comp. Multiphase Flows*, 2(3), 179-188.

FENG, Y.Q., SCHWARZ, M.P., YANG, W. and COOKSEY, M.A., (2015), "Two-phase CFD model of the bubble-driven flow in the molten electrolyte layer of a Hall-Héroult aluminum cell", Metall and Materi Trans B., 46, 1959-1981.

WANG, Y. F. and ZHANG, L. F., "Numerical modelling on the fluid flow-related phenomena in an aluminium electrolysis cell", Light Metal 2010, 14.

ZHANG, K., FENG, Y.Q., SCHWARZ, P., WANG, Z. and COOKSEY, M., (2013), "Computational fluid dynamics (CFD) modeling of bubble dynamics in the aluminum smelting process", *Ind. Eng. Chem. Res.*, 52 (33), 11378–11390.

ZHAO, Z.B., GAO, B.L., WANG, Z.W., HU, X.W., FENG, Y.Q., (2016a), "Anodic Bubble Behaviour and Voltage Drop in a Laboratory Transparent Aluminium Electrolytic Cell", METALLURGICAL AND MATERIALS TRANSACTIONS B, 47B, 1962-1975

ZHAO, Z.B., FENG, Y.Q., SCHWARZ, M.P., WITT, P.J., WANG, Z.W. and COOKSEY, M., (2016b), "Numerical modeling of flow dynamics in the aluminum smelting process: Comparison between Air–Water and CO2–Cryolite systems", *Metall and Materi Trans B*, 2016.